Reduction of Transmission Power Error and Current for Dual Active Bridge DC-DC Converter in Energy Storage Systems

Jun-ichi Itoh, Kengo Kawauchi, Hiroki Watanabe, Keisuke Kusaka
Dept. of Electrical, Electronics and Information Engineering
Nagaoka University of Technology
Niigata, Japan
itoh@vos.nagaokaut.ac.jp, k_kawauchi@stn.nagaokaut.ac.jp, hwatanabe@vos.nagaokaut.ac.jp, kusaka@vos.nagaokaut.ac.jp

Abstract— **This paper proposes a control method for a dual active bridge (DAB) converter, which achieves both a reduction method of a non-linear transmission power error and an inductor current reduction with a three-level operation. The non-linear transmission power error is compensated by designing a zero current period in the inductor current by the three-level operation. In addition, the inductor current reduction method for the three-level operation is also proposed. In the non-linear transmission power error compensation method, the inductor current is reduced by suppressing the circulating current with determining zero-current period to be the dead-time. The validity of the proposed method is confirmed by a 2-kW prototype. As the experimental results, the transmission power error is reduced by up to 85.1%. Moreover, the inductor current is reduced by up to 64.1% and loss is reduced by up to 58.6%.**

Keywords— Dual active bridge converter; Dead-time error; Current reduction; Three-level operation

I. INTRODUCTION

In recent years, a DC micro-grid system has been actively studied in order to solve the environmental problems [1-5]. An isolated bi-directional DC-DC converter is required for energy storage systems in order to control power between the DC bus and the energy storage systems with galvanic isolation. In the isolated bi-directional DC-DC converter, a dual active bridge (DAB) converter is generally employed for these applications because the DAB converter obtains high efficiency because of achieving zero voltage switching (ZVS) without additional components [6-10]. However, a non-linear transmission error occurs due to the dead-time at light load although the DAB converter has to operate at a wide load range in energy storage systems [11]. In order to reduce the error of the transmission power, the dead-time compensation method has been proposed [12]. In [12], the dead-time error is compensated by the feedforward compensation that subtracts the dead-time from the command of the phase-shift between the primary and the secondary output voltage. However, this conventional method is effective only when the transmission-power error is linear. The non-linear error due to a voltage-polarity-reversal phenomenon is not compensated by the compensation method in [12].

The authors have proposed the non-linear dead-time compensation method using a three-level operation [13]. By applying the compensation method in [13], the non-linear transmission error is compensated although an inductor current is increased by a circulating current owing to the three-level operation. The circulating current should be suppressed because the increase in the inductor current causes the decrease of efficiency.

This paper proposes the compensation method of the non-linear transmission error with the current reduction method in the three-level operation. The contribution of this proposed method is to overcome the problems of the conventional compensation method that is the increase in loss due to the circulating current. The transmission power error is compensated by avoiding the voltage-polarity-reversal. In addition, the inductor current is reduced by suppressing the circulating current with determining the zero-current period to be the dead-time. By applying the proposed method, the energy storage system is operated without the dead-time error with high efficiency.

This paper is organized as follows; firstly, the conventional control method is discussed. Secondly, the reduction method of non-linear transmission power error is introduced. Next, the current reduction method for the three-level operation is proposed. Finally, experiments are conducted in order to verify the compensation method of the non-linear transmission power error caused by the dead-time and the current reduction method for the three-level operation.

II. CONVENTIONAL CONTROL METHOD

A. Traditional two-level operation method

Fig. 1 shows the circuit configuration of the DAB converter. The DAB converter consists of two H-bridge inverters, an additional inductor, and a high-frequency transformer. The primary and the secondary inverters generate the square-wave voltage, and the transmission power is controlled by a phase-shift δ between each inverter output voltage called the single phase shift (SPS) control. The transmission power is expressed by [12],

$$P = \frac{NV_{in}V_{out}}{\omega L}\delta\left(1-\frac{|\delta|}{\pi}\right) \quad (1),$$

where ω is a switching angular frequency, L is an additional inductor, N and δ are turn ratio and phase-shift between the primary inverter output voltage v_{pr} and the inverter on the secondary side output voltage v_{se}.

Fig. 2 shows the two-level operation waveform with and without the dead-time. In the case of taking no account of the dead-time, the transmission power is controlled by the phase-shift δ without the transmission-power error. However, in an actual system, the dead-time is needed in order to prevent two switching devices from the short circuit. In this case, the transmission-power error occurs at light load when the inductor current becomes zero during the dead-time. The inductor current is clamped to zero because the inductor current does not conduct primary inverter during the dead-time. As a result, the polarity of the primary inverter output voltage is reversed by the clamped inductor current. Consequently, the transmission-power error is caused by the voltage-polarity-reversal phenomenon due to the dead-time [11].

Fig. 3 shows the influence of the voltage-polarity-reversal phenomenon for the transmission power. The transmission power error caused by the voltage-polarity-reversal phenomenon is not compensated by the conventional feedforward method because the transmission power error due to the dead-time varies depending on the width of the voltage-polarity-reversal [11–12]. The period of the voltage-polarity reversal is varied by the relationship between the inductor current and the dead-time period [11]. At the period between $2\delta_{dt}$ and δ_{dt}, the transmission power error is varied corresponding the width of the voltage-polarity-reversal, where δ_{dt} is the dead-time in the radian calculated as (2) using the dead-time T_{dt} and switching angular frequency ω,

$$\delta_{dt} = \omega T_{dt} \quad (2).$$

After δ_{dt}, the transmission-power error becomes the constant value of the dead-time without the voltage-polarity reversal. In the area where the phase-shift δ is smaller than the dead-time δ_{dt}, power is not transferred because the phase-shift δ is canceled by the dead-time [12].

B. *Non-linear Transmission Power Error Compensation Method*

1) Conventional operation method

Fig. 4 shows the operation waveforms of the conventional three-level mode. In the conventional operation method, the zero voltage phases of each inverter are controlled identically with the phase-shift δ as a constant. The three-level modes are considered under the condition of $V_{in} = NV_{out}$ and $\varepsilon = \gamma$. Note that the parasitic capacitance and the magnetizing current are not considered in this calculations. Under the steady state condition, the inductor current i_{L1} at the switching moment as follows,

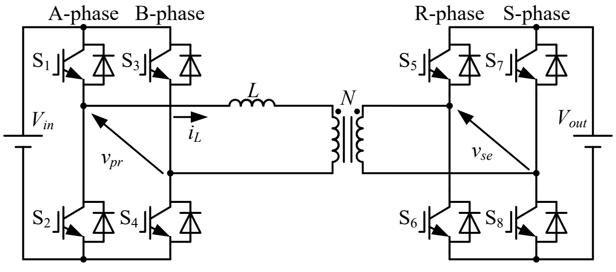

Fig. 1. Dual active bridge converter.

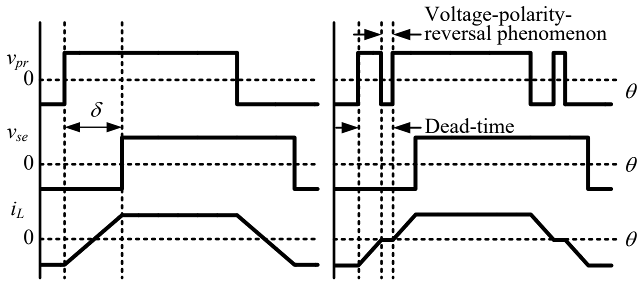

(a) Without dead-time. (b) With dead-time.

Fig. 2. Operation waveform with conventional two-level operation.

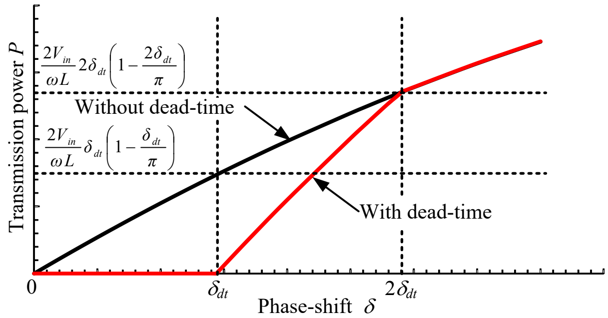

Fig. 3. Influence of dead-time for transmission power.

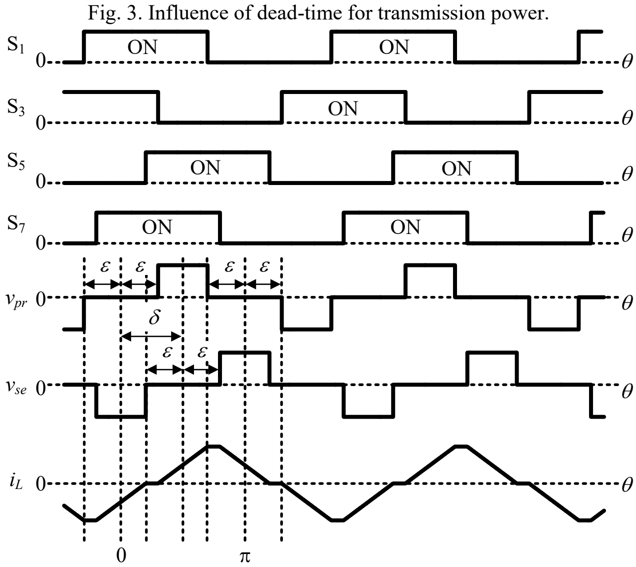

Fig. 4 Conventional operation waveform.

$$
i_{LI}(\theta)=\begin{cases}\frac{V_{in}}{\omega L}(\theta-\delta+\varepsilon) & (0\le\theta\le\delta-\varepsilon)\\ 0 & (\delta-\varepsilon\le\theta\le\varepsilon)\\ \frac{V_{in}}{\omega L}(\theta-\varepsilon) & (\varepsilon\le\theta\le\pi-\varepsilon)\\ \frac{V_{in}}{\omega L}(\pi-2\varepsilon) & (\pi-\varepsilon\le\theta\le\delta+\varepsilon)\\ \frac{V_{in}}{\omega L}(\pi-\theta-\varepsilon+\delta) & (\delta+\varepsilon\le\theta\le\pi)\end{cases} \quad (3).
$$

According to (3), the transmission power P_I is calculated by

$$
P_I=\frac{2}{2\pi}\int_0^{\pi} v_{pr}(\theta)i_{LI}(\theta)d\theta=\frac{V_{in}^2}{2\pi\omega L}(\pi-2\varepsilon)^2 \quad (4).
$$

In order to be operated by the conventional three-level mode, PWM pulses of each inverter output voltage are not overlapped. The condition of the conventional three-level mode is expressed by

$$
2\varepsilon\ge\pi-\delta \quad (5).
$$

2) Dead-time influence and compensation of three-level mode

Fig. 5 shows the dead-time effect on the primary inverter output voltage and the inductor current of the three-level mode. The voltage-polarity-reversal phenomenon is eliminated by determining the zero-current period ϕ to become longer than the dead-time because the voltage-polarity-reversal phenomenon occurs when the inductor current becomes zero during the dead-time. The condition of $\phi\ge\delta_{dt}$ is given by

$$
\varphi=2\varepsilon-\delta\ge\delta_{dt} \quad (6).
$$

However, the duty of the primary inverter output voltage is decreased by the dead-time because diodes of the B-phase leg is not conducted during the dead-time instead of designing the zero-current period ϕ to be longer than the dead-time. Therefore, the duty of primary inverter output voltage is needed to be compensated.

Fig. 6 shows the dead-time compensation for the three-level operation. The duty error by the dead-time is compensated by (7) because the decrease of the duty affects the phase-shift δ and the zero voltage phase ε,

$$
\begin{cases}\delta^*=\delta+\delta_{dt}/2\\ \varepsilon^*=\varepsilon-\delta_{dt}/2\\ \gamma^*=\varepsilon\end{cases} \quad (7),
$$

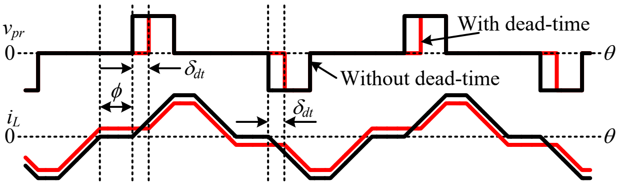

Fig. 5. Dead-time effect of three-level mode.

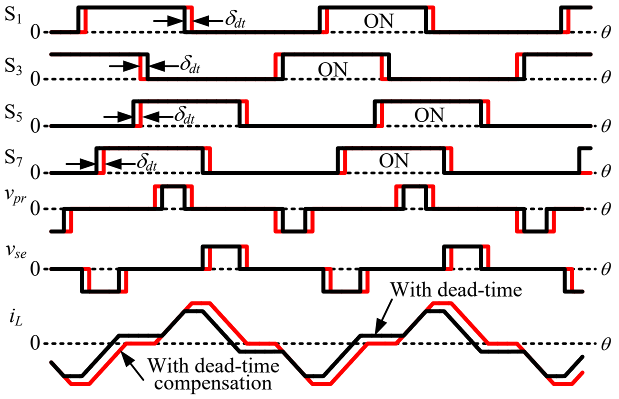

Fig. 6. Dead-time compensation mehod for three-level operation.

where δ^*, ε^* and γ^* are the phase-shift commands, the zero voltage phase command of the primary inverter, and the zero voltage phase command of the secondary inverter.

3) Decision of phase-shift δ

In this chapter, the phase-shift δ is determined as transferring maximum power in order to compensate the entire range of transmission power error. According to (4) and (5), the maximum transmission power is given by minimizing the zero voltage phase ε. Therefore, the phase-shift δ of the maximum transmission power δ_{max_I} is given by (8) using (5) and (6),

$$
\delta_{\max I}=\frac{1}{2}(\pi-\delta_{dt}) \quad (8).
$$

Therefore, the range of the zero voltage phase ε and the transmission power of P_I are expressed by (9) and (10) using (4), (5), and (6),

$$
\frac{1}{4}(\pi+\delta_{dt})\le\varepsilon\le\frac{1}{2}\pi \quad (9),
$$

$$
0\le P_I\le\frac{V_{in}^2}{4\pi\omega L}(\pi-\delta_{dt})^2 \quad (10).
$$

In addition, RMS value of the inductor current is expressed by (11) from (3),

$$
\begin{aligned} i_{LI\_RMS}&=\sqrt{\frac{2}{2\pi}\int_0^{\pi} i_{LI}(\theta)^2 d\theta}\\ &=\frac{V_{in}}{\omega L}\sqrt{\frac{1}{3\pi}(2\varepsilon-\pi)^2(3\delta-\pi+2\varepsilon)}\end{aligned} \quad (11).
$$

III. Current Reduction Method for Three-level Operation

Figure 7 shows the circulating current of the conventional three-level operation. In the conventional three-level operation, the circulating current accounts for more than half of the inductor current. Therefore, conduction loss increases because the inductor current against the transmission power is bigger than the two-level mode. Hence, the circulating current is required to reduce in order to achieve high efficiency.

Figure 8 shows waveforms of the proposed three-level operation. In the proposed operation method, the zero voltage phases of each inverter and the phase-shift are controlled in a different manner of the conventional three-level operation. The proposed three-level modes is considered under the condition of $V_{in} = NV_{out}$ and $\varepsilon = \gamma$. Note that, the parasitic capacitance and the magnetizing current are not considered in this calculations. Under the steady state condition, the inductor current i_{LII} at the switching moment as follows,

$$i_{LII}(\theta)=\begin{cases} 0 & (0 \le \theta \le \varepsilon) \\ \dfrac{V_{in}}{\omega L}(\theta-\varepsilon) & (\varepsilon \le \theta \le \varepsilon+\delta) \\ \dfrac{V_{in}}{\omega L}\delta & (\varepsilon+\delta \le \theta \le \pi-\varepsilon) \\ \dfrac{V_{in}}{\omega L}(\pi-\varepsilon+\delta-\theta) & (\pi-\varepsilon \le \theta \le \pi-\varepsilon+\delta) \\ 0 & (\pi-\varepsilon+\delta \le \theta \le \pi) \end{cases} \quad (12).$$

Then, the transmission power P_{II} is given by (13) using (12),

$$P_{II} = \frac{2}{2\pi}\int_0^{\pi} v_{pr}(\theta) i_{LII}(\theta) d\theta = \frac{V_{in}^2}{2\pi\omega L}\delta(2\pi - 4\varepsilon - \delta) \quad (13).$$

In order to be operated by the proposed three-level mode, pulses of each inverter output voltage are overlapped. The condition of the proposed three-level mode is expressed by

$$2\varepsilon < \pi - \delta \quad (14).$$

In addition, the RMS value of the proposed three-level operation is given by (15), from (12),

$$\begin{aligned} i_{LII\_RMS} &= \sqrt{\frac{2}{2\pi}\int_0^{\pi} i_{LI}(\theta)^2 d\theta} \\ &= \frac{V_{in}}{\omega L}\sqrt{\frac{1}{3\pi}(2\varepsilon-\pi)^2(3\delta-\pi+2\varepsilon)} \end{aligned} \quad (15).$$

Figure 9 shows the circulating current of the proposed three-level operation. In order to reduce the inductor current in the three-level mode, the circulating current is suppressed by minimizing the phase-shift angle and zero-voltage periods

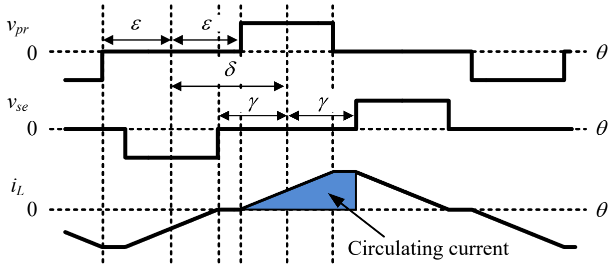

Fig. 7. Circulating current of conventional three-level mode.

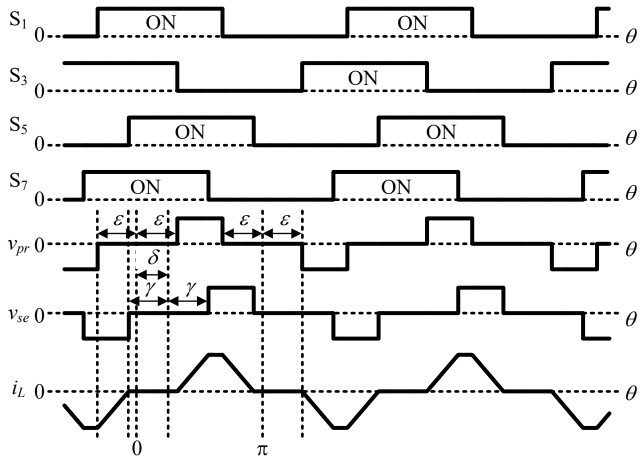

Fig. 8. Proposed operation waveform.

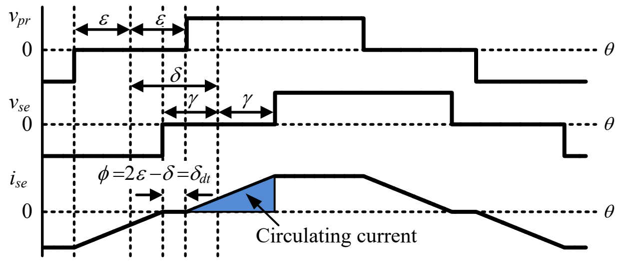

Fig. 9. Circulating current of proposed three-level operation.

regarding the transmission power. The phase-shift and zero-voltage periods are minimized when the zero-current period ϕ is the same as the dead-time. Therefore, the inductor current is reduced by controlling the zero-current period ϕ to be the dead-time period δ_{dt}. The condition of $\phi = \delta_{dt}$ is given by

$$\varepsilon = \frac{1}{2}(\delta + \delta_{dt}) \quad (16).$$

Substituting (16) for (13), the transmission power P_{III} is expressed by

$$P_{III} = \frac{V_{in}^2}{2\pi\omega L}\delta(2\pi - 2\delta_{dt} - 3\delta) \quad (17).$$

The command of the phase-shift δ^* is given by solving (17) for the phase-shift δ as

$$\delta^* = \frac{(2\pi - 2\delta_{dt}) - \sqrt{(2\pi - 2\delta_{dt})^2 - 24\pi\omega LP^*/V_{in}^2}}{6} \quad (18),$$

where P^* is the command of the transmission power. Using (16) and (18), the inductor current is reduced because the circulating current is suppressed.

Figure 10 shows the flowchart for the determination of operation modes. The operation mode is determined as follows; the phase-shift angle δ is calculated with the transmission power command P^* by solving (1) for the phase-shift

$$\delta = \frac{\pi - \sqrt{\pi^2 - 4\pi\omega LP^*/V_{in}^2}}{2} \quad (19).$$

The operation mode is decided by the phase-shift command δ^* and the dead-time δ_{dt}. Under the condition of $\delta^* > 2\delta_{dt}$, the conventional two-level operation is used. In contrast, the transmitted power is determined by the phase-shift δ and the zero-voltage period ε given by (16) and (18) when the three-level operation is used. The voltage-polarity-reversal phenomenon occurs when the phase-shift angle δ reaches δ_{dt} because the inductor current reaches zero during the dead-time. Therefore, the phase shift angle is limited by $\delta_{dt} + \alpha$ where α is a few margin to avoid the voltage-polarity-reversal phenomenon. The margin α is needed to be design as small as possible because the circulating current increases as the margin α is larger. When an FPGA is used for an experiment, the margin α is determined as one clock of the FPGA because the phase-shift is controlled by the clock period of the FPGA. After the operation range of $\delta_{dt} + \alpha$, the transmission power is controlled by the zero-voltage periods with the phase-shift of $\delta_{dt} + \alpha$. The zero-voltage command is given by (20) form (17) and $\delta_{dt} + \alpha$,

$$\varepsilon = \frac{1}{2}\left\{2\pi - (\delta_{dt} + \alpha) - \frac{2\pi\omega LP^*}{(\delta_{dt} + \alpha)V_{in}^2}\right\} \quad (20).$$

Finally, the dead-time error due to avoiding the voltage-polarity-reversal phenomenon is compensated by (7).

IV. Experimental Results

Table I shows the experimental parameters. A 2-kW prototype of the DAB converter is tested in order to confirm the validity of the proposed method.

Figure 11 shows experimental waveforms of the two-level mode and three-level modes. Fig. 11(a) shows operation waveforms of two-level mode. The transmission error of 47.6% occurs because the voltage-polarity-reversal phenomenon is caused. By applying the conventional non-linear dead-time compensation method, the transmission error is reduced by 44.9%. However, the inductor is 11.3 A due to the circulating current. In contrast, using the proposed current reduction method, the inductor current against the transmission power is

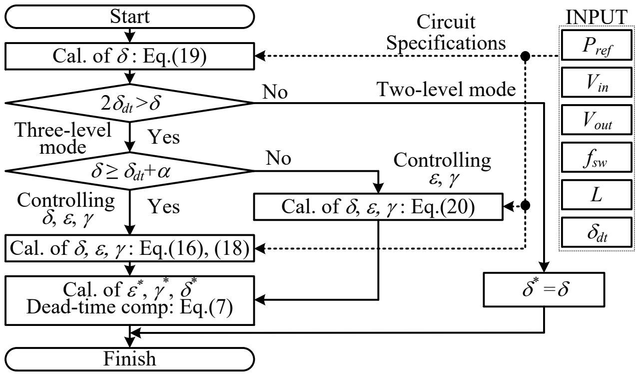

Fig. 10. Flowchart of determination of operation modes.

Table I. Experimental condition.

Input voltage V_{in}	240 V	Additional inductance L	128 μH
Output voltage V_{out}	240 V	Margin of dead-time α	0.36deg
Rated power P	2 kW	Transformer turn ratio N	1
Dead time T_{dt}	2.1 μs	Switching frequency f_{sw}	20 kHz

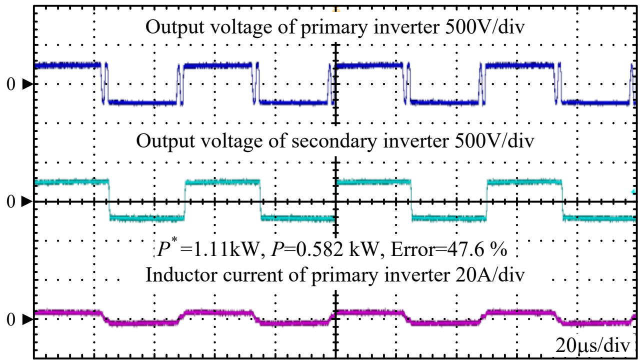

(a) Two-level mode.

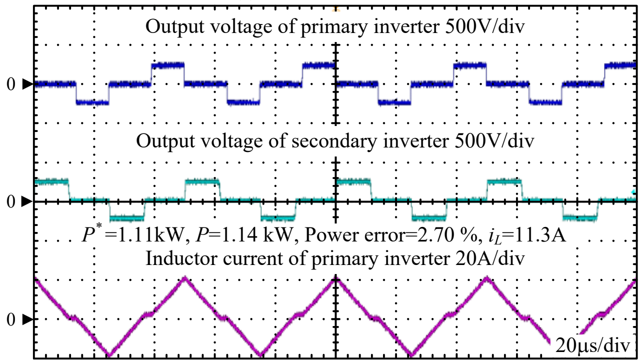

(b) Conventional three-level mode.

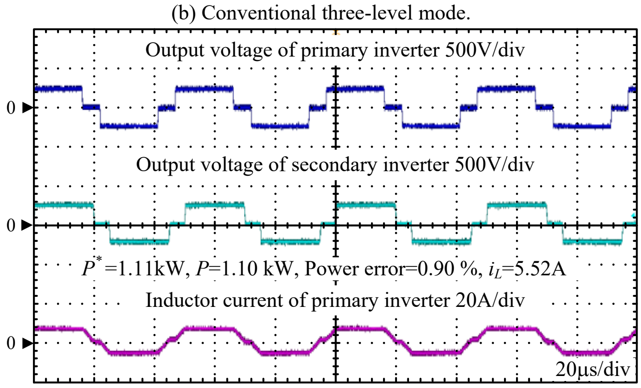

(c) Proposed three-level mode.

Fig. 11. Experimental waveforms of two-level operation and three-level operation.

reduced by 51.2% by controlling the zero-current period to the dead-time δ_{dt}.

Figure 12 shows the characteristics of the transmission power against the transmission power command. In the two-level mode, the transmission power has the non-linear error due to the voltage-polarity-reversal phenomenon. By applying the proposed method, the transmission-power error is reduced by up to 81.5% by avoiding the voltage-polarity-reversal phenomenon.

Figure 13 shows the characteristics of the inductor current regarding the transmission power. By applying the conventional method, the inductor current is increased by more than twice that of the two-level mode. On the other hand, the inductor current is reduced by up to 64.1% because the circulating current is reduced with the proposed method.

Figure 14 shows the efficiency characteristics of the two-level mode, the conventional method, and the proposed method. In the conventional method, the efficiency is decreased owing to the increase in conduction loss. By applying the proposed method, loss is reduced by up to 58.6% because the increase in the inductor current is suppressed.

V. Conclusion

This paper proposed the compensation method of the transferred power error due to the dead-time with the reduction method for the inductor current. The error of the transmission power is reduced by up to 85.1% because the voltage-polarity-reversal phenomenon is avoided. Moreover, the inductor current is reduced by up to 64.1%. In the future work, the compensation method for the non-linear dead-time error under the condition of $V_{in} \neq NV_{out}$ will be considered.

References

[1] M. Mao, Z. Dong, L. Chang: "Accurate Output Power Control of Converters for Micrograds Based on Local Measurement and Unified Control", IEEJ Journal of Industry Applications, Vol. 4, No. 4, pp.331-338, 2015.

[2] H. Kakigano, Y. Toshifumi: "Low-Voltage Bipolar-Type DC Microgrid for Super High Quality Distribution", IEEE Trans. on Power Electronics, Vol. 25, No. 12, pp.3066-3075, 2010.

[3] J. M. Guerrero, J. C. Vasquex, J. Matas, L. G. Vicuna, M. Castilla: "Hierarchical Control of Droop-Controlled AC and DC Microgrids—A General Approach Toward Standardization", IEEE Trans. on Industry Applications, Vol. 58, No. 1, pp.158-172, 2011.

[4] X. Liu, P. Wang and P. C. Loh, "A Hybrid AC/DC Microgrid and Its Coordination Control," in IEEE Transactions on Smart Grid, vol. 2, no. 2, pp. 278-286, June 2011.

[5] B. Zhao, Q. Song, W. Liu and Y. Xiao, "Next-Generation Multi-Functional Modular Intelligent UPS System for Smart Grid," in IEEE Transactions on Industrial Electronics, vol. 60, no. 9, pp. 3602-3618, Sept. 2013.

[6] H. Zhou, A. M. Khambadkone: "Hybrid Modulation for Dual-Active-Bridge Bidirectional Converter With Extended Power Range for Ultracapacitor Application", IEEE Trans. on Industry Application, Vol. 29, No. 4, pp.1667-1680, 2014.

[7] Felix J. and Jurgen B., "Generalized Modeling and Optimization of a Bidirectional Dual Active Bridge DC-DC Converter Including Frequency Variation", IEEJ Journal of Industry Applications, Vol.4, No.5, pp.593-601, 2015.

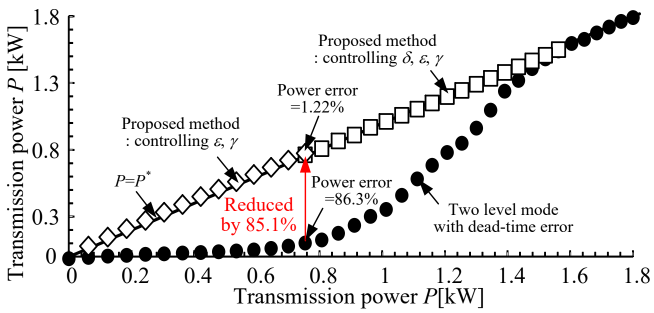

Fig. 12. Charactarisitics of transmission power.

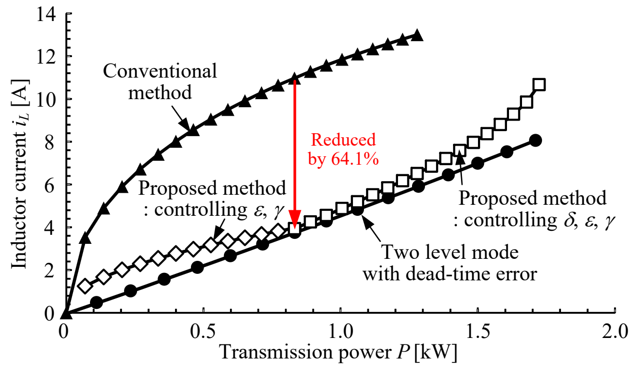

Fig. 13. Charactaristics of inductor curretn regarding transmission power.

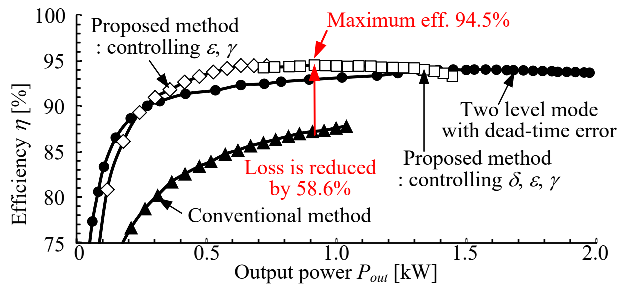

Fig. 14. Efficiency charactaristics of conventional method and proposed method.

[8] H. Higa and J. Itoh, "Zero voltage switching over entire load range and wide voltage variation of parallelly-connected dual-active-bridge converter using power-circulating operation," 2017 IEEE 3rd International Future Energy Electronics Conference and ECCE Asia (IFEEC 2017 - ECCE Asia), Kaohsiung, 2017, pp. 506-511.

[9] G. Guidi, A. Kawamura, Y. Sasaki and T. Imakubo, "Dual active bridge modulation with complete zero voltage switching taking resonant transitions into account," Proceedings of the 2011 14th European Conference on Power Electronics and Applications, Birmingham, 2011, pp. 1-10.

[10] M. Nakahara, K. Wada: "Loss Analysis of Magnetic Components for a Solid-State-Transformer", IEEJ Journal of Industry Applications, Vol. 4, No. 4, pp.387-394, 2015.

[11] B. Zhao, Q. Song, W. Liu, Y. Sun: "Dead-time Influence of the High-Frequency Isolated Bidirectional Full-Bridge DC–DC Converter: Comprehensive Theoretical Analysis and Experimental Verification", IEEE Trans. on Power Electronics, Vol. 29, No. 4, pp.1667-1680, 2014.

[12] K. Takagi and H. Fujita, "Dynamic control and dead-time compensation method of an isolated dual-active-bridge DC-DC converter," 2015 17th European Conference on Power Electronics and Applications (EPE'15 ECCE-Europe), Geneva, 2015, pp. 1-10.

[13] J. Itoh, K. Kawauchi, H. Higa, " Dead-time Compensation with DC Offset Current Elimination Method using Three-level Operation for Dual Active Bridge DC-DC Converter," 2018 IEEE Energy Conversion Congress and Exposition (ECCE), Portland, OR, 2018.